SIMULATION OF MARINE ADVECTION FOG WITH THE CALSPAN ADVECTION FOG MODEL USING PROGNOSTIC EQUATIONS FOR TURBULENT ENERGY

CALSPAN CORPORATION

PREPARED FOR
NAVAL AIR SYSTEMS COMMAND

JUNE 1976

Calspan

SIMULATION OF MARINE ADVECTION FOG WITH THE CALSPAN ADVECTION FOG MODEL USING PROGNOSTIC EQUATIONS FOR TURBULENT ENERGY

by

Eugene J. Mack and C. William Rogers

Calspan Report No. CJ-5756-M-2

Project Sea Fog
Fourth Annual Summary Report

Part 2

Prepared For:

NAVAL AIR SYSTEMS COMMAND
WASHINGTON, D.C. 20360
CODE AIR-370C

CONTRACT NO. N000019-75-C-0508
JUNE 1976

Calspan Corporation
Buffalo, New York 14221

APPROVED FOR PUBLIC RELEASE:
DISTRIBUTION UNLIMITED

TABLE OF CONTENTS

Section		Page
1	INTRODUCTION AND SUMMARY	1
2	RESULTS OF SIMULATIONS OF MARINE ADVECTION FOG	4
	2.1 The Influence of Radiative Transfer on Fog Development	4
	2.2 The Influence of a Warming Sea Surface on the Development of Advection Fog	10
3	COMPARISON OF A NUMERICAL SIMULATION OF ADVECTION FOG WITH A FOG EVENT OBSERVED OFF THE COAST OF NOVA SCOTIA	15
	3.1 Observations of a Marine Advection Fog	15
	3.2 Numerical Simulations of Fog Formed by Turbulent Heat Exchange with a Cold Sea Surface and Comparison with Observations	21
	REFERENCES	25
	APPENDIX A -- FORTRAN LISTING OF COMPUTER PROGRAM WITH COMMENT CARDS FOR THE CALSPAN TWO-DIMENSIONAL ADVECTION FOG MODEL	A-1

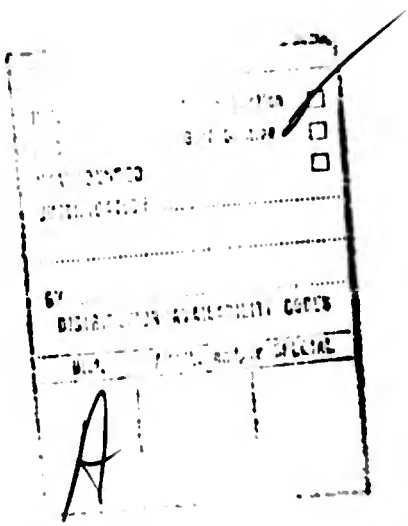

LIST OF FIGURES

Figure No.		Page
1	Contours of LWC (g m^{-3}) and the Vertical Temperature Profile for an Advection Fog Simulation by a Numerical Model Using Prognostic Equations for Turbulent Energy and a Radiative Absorption Coefficient Dependent on a Monodisperse Droplet Population.....	8
2	Contours of LWC (g m^{-3}) and the Vertical Temperature Profile for an Advection Fog Simulation by the 1976 Calspan Model Using Prognostic Equations for Turbulent Energy and a Radiative Absorption Coefficient Dependent on a Spectrum of Droplets.....	9
3	Contours of LWC (g m^{-3}) and the Vertical Temperature Profile for a Numerical Simulation of the Vertical Development of an Advection Fog Over 2C Warmer Water by the 1976 Calspan Model.	12
4	Contours of LWC (g m^{-3}) and the Vertical Temperature Profile for a Numerical Simulation of the Vertical Development of an Advection Fog Over 5C Warmer Water by the 1976 Calspan Model.	14
5	Sketch of the Vertical Profile of the Fog of 1915-0040, 2-3 August 1975.....	16
6	Contours of Visibility (m) for the Fog of 1915-0040 EDT, 2-3 August 1975.....	17
7	Sea Surface Isotherm (C) Chart for the Fog of 1915-0040, 2-3 August 1975.....	18
8	Selected Vertical Temperature Profiles In and Around the Fog of 2-3 August 1975.....	19
9	Results of Numerical Simulation of Marine Advection Fog Using Three Versions of the Calspan Advection Fog Model.....	22

Section 1

INTRODUCTION AND SUMMARY

Under previous joint sponsorship of the Naval Air Systems Command and the National Aeronautics and Space Administration, Calspan Corporation developed a two-dimensional model of advection fog (Mack et al., 1972) in conjunction with a field investigation of coastal fogs. Recently under sponsorship of NASA, the model was improved (Rogers et al., 1975) by incorporating prognostic equations for the horizontal wind with the objective of employing turbulent exchange coefficients in the model which would respond to both the predicted wind shear and temperature gradients in a more realistic manner. The 1975 version of the model predicts the evolution of potential temperature, horizontal wind, water vapor content, and liquid water content in a vertical cross section of the atmosphere as determined by the processes of vertical turbulent transfer and horizontal advection, as well as radiative cooling and drop sedimentation in fog. The model simulates the formation or dissipation of advection fog in response to the transfer of heat and moisture between the atmosphere and surface as forced by advection over horizontal variations in the surface temperature. The model was fully described by Rogers et al. (1975), and details will not be repeated here.

As Task II under Contract No. N00019-75-C-0508 from the Naval Air Systems Command, the objective of this year's limited investigation was to develop more realistic descriptions of turbulent transfer and radiative processes within the boundary layer framework of the Calspan advection fog model, thereby providing a sound basis for incorporation of dynamic influences in future studies. To achieve this objective, the numerical modeling study was closely guided by the observational program. Observational data from West Coast field studies were used to select initial and boundary conditions for model simulations, as well as to validate the model predictions. The improved version of the advection fog model was then applied to investigate the influence of a sequence of sea surface temperature variations of the type observed to be associated with marine fog formation off the California coast (Mack et al.,

1973; 1974; 1975). The model was also applied to simulate the shallow type of advection fog observed off the coast of Nova Scotia by Mack and Katz (1976).

During the investigation, programming and testing of the improvements to the advection fog model was carried out. A prognostic equation for the turbulent energy has been incorporated in the model, and the turbulent exchange coefficients are computed from the turbulent energy. A Fortran listing (with comment cards) of the computer program as it is now constituted is provided in Appendix A.

Numerical simulations of marine fog formation resulting from advection of nearly-saturated air over colder water have been carried out. It has been demonstrated that if a shallow marine fog (formed by the advection of nearly-saturated air over colder water) is subsequently advected over warmer water, significantly greater vertical development of the fog may result. These results are discussed in Section 2.

Investigation of influences of alternative parameterizations of radiative cooling on the predicted development of marine fog has shown that, in agreement with results from Calspan observation studies of marine fog, radiative cooling plays a crucial role in the vertical development and persistence of marine fog. The results of these simulations are also discussed in Section 2.

In Section 3, simulations of advection fog from both the upgraded Calspan model (Appendix A) and the 1975 version of the model (Rogers et al., 1975) are compared. In addition, these simulations are compared with a marine advection fog observed off the coast of Nova Scotia (Mack and Katz, 1976).

The results obtained from the upgraded model show better agreement with the Calspan observational studies of marine fog. However, a principal area of disagreement remains that of the magnitude of water temperature changes required in the model to initiate marine fog formation. Recent observations

off the coast of Nova Scotia show that sea surface temperature gradients of 2-4°C per 10 km may be responsible for triggering fog in some instances. Off the West Coast, fogs formed by direct cooling from below have not yet been observed. The model, however, requires sea surface temperature changes of the order of 5-6°C to form fog of realistic depths. Additional numerical experimentation will be required to determine whether differences between the turbulent exchange coefficients for heat and moisture, or perhaps even dynamic influences, can resolve the differences between the model and the available observations.

Section 2

RESULTS OF SIMULATIONS OF MARINE ADVECTION FOG

To facilitate this investigation of marine fog formation and to provide a better simulation of the subsequent vertical development of fog under the influences of radiative cooling and sea surface temperature distributions, a more realistic description of turbulent transfer was incorporated into the model. This was formulated by incorporating a prognostic equation for turbulent energy and computing turbulent exchange coefficients from the predicted turbulent energy (Pepper and Lee, 1974). The primary goal in making such a change was to produce a representation of turbulent transfer in the model which realistically describes turbulent transfer above a surface layer cooled from below. This capability was required to overcome the artificial suppression of turbulence aloft caused by the extreme stability of the surface layer. (See Appendix A for details of the upgraded version of the Calspan advection fog model.)

2.1 The Influence of Radiative Transfer on Fog Development

The treatment of radiation in the 1975 version of the model was designed to capture the essence of physical processes while avoiding detailed radiative transfer calculations. In the absence of fog, the radiative flux divergence $\frac{\partial R}{\partial z}$ is assumed to be everywhere zero. In the presence of fog, a radiative flux divergence representing the absorption and radiation of infrared radiation by fog drops is introduced. An approximation expression relating the radiative flux divergence $\frac{\partial R}{\partial z}$ to the vertical distribution of the liquid water mixing ratio $w(z)$ in the model is obtained by employing a spectrally-averaged mass absorption coefficient k_w to represent the influences of fog on radiative transfer. For simplicity, the fog is assumed to be at the absolute temperature T_0 of the surface, thereby neglecting the influences of temperature gradients on the radiative transfer in the model fog.

It is assumed that a radiation flux equal to the black body radiation from the surface is transferred upward through the fog or

$$R_u(z) = \sigma T_o^4 \quad . \tag{1}$$

Under clear sky conditions, it is also assumed that a downward flux of back radiation from the atmosphere equal to approximately 75% of the black body radiation from the surface is incident on the fog top at height z_T (Sutton, 1953) or

$$R_d(z_T) = .75\sigma T_o^4 \tag{2}$$

This downward flux of radiation on the fog top from the atmosphere is deficient in energy in the water vapor window portion of the spectrum between approximately 8.5 and 12 μm wavelength.

Inside the fog, the downward flux of radiation is determined by absorption and radiation of energy by the fog. At height z in the fog, the downward flux of radiation is

$$\begin{aligned} R_d(z) &= .75\sigma T_o^4 \exp\left[-1.6\int_z^{z_T} k_w(z')\rho w(z')dz'\right] \\ &\quad + \sigma T_o^4 \int_z^{z_T} 1.6\, k_w(\zeta)\, \rho w(\zeta) \exp\left[-1.6\int_z^{\zeta} k_w(z')\rho w(z')dz'\right]d\zeta \\ &= \sigma T_o^4 \left\{1 - .25\exp\left[-1.6\int_z^{z_T} k_w(z')\rho w(z')dz'\right]\right\} \end{aligned} \tag{3}$$

The first term on the right represents the downward flux of radiation incident on the fog top as attenuated through absorption by the fog in the distance from z_T to z. In the second term on the right, the downward radiation reaching height z due to radiation from an element of fog of thickness $d\zeta$ at height ζ is integrated from height z to the fog top at height z_T. Here the product $\rho w(z)$ of the density of air times the liquid water mixing ratio is the liquid water content of the model fog at height z. The influence of the angular dependence of the radiation field has been approximated by increasing the optical path lengths by the diffusivity factor 1.6 (Goody, 1964).

The net radiative flux at height z in the fog becomes

$$R(z) = R_u(z) - R_d(z) = .25\sigma T_o^4 \exp[-1.6\int_z^{z_T} k_w(z')\rho w(z')dz'] \qquad (4)$$

Differentiating with respect to z, we obtain the expression used in the model for the radiative flux divergence produced by fog

$$\frac{\partial R}{\partial z}(z) = .25\sigma T_o^4 1.6 k_w(z)\rho w(z)\exp[-1.6\int_z^{z_T} k_w(z')\rho w(z')dz'] \qquad (5)$$

To determine the form for the mass absorption coefficient k_w employed in the model, we must consider the absorption cross sections of fog drops. For fog drops of radius greater than approximately 4.5 μm, Zdunkowski and Nielson (1969) have shown that the spectrally-averaged absorption cross section of a fog drop for black body radiation is within 20% of πr^2, where r is the radius of the drop. For a fog drop concentration of N drops per unit volume, the absorption per unit length in the model fog is assumed to be

$$1.6\ k_w \rho w = 1.6\ N\pi r^2 \qquad (6)$$

where r is the mean volume radius of the fog drops.

Solving for the mean fog drop radius r from the relation

$$N\rho_l \frac{4\pi}{3} r^3 = \rho w \qquad (7)$$

we obtain

$$r = (\frac{3\rho w}{4\pi\rho_l N})^{\frac{1}{3}} \qquad (8)$$

Substituting for r in Eq. (6), we obtain the expression

$$1.6\ k_w \rho w = 1.6(\pi N)^{\frac{1}{3}}(\frac{3}{4\pi\rho_l})^{\frac{2}{3}}(\rho w)^{\frac{2}{3}} \qquad (9)$$

for the absorption per unit path length in the fog.

Assuming a constant drop concentration of N = 50 drops per cm^3, reasonably representative of coastal advection fogs (Mack et al., 1975), Eq. (9) reduces to expression

$$1.6\ k_w \rho w = 7.1(\rho w)^{\frac{2}{3}} cm^{-1} \tag{10}$$

for the absorption per cm employed in the fog model as a function of the predicted liquid water content ρw in grams per cm^3. To calculate the radiative flux divergence $\frac{\partial R}{\partial z}$ in the potential temperature equation of the model, the quantity $1.6\ k_w(z)\rho w(z)$ in Eq. (5) is replaced by $7.1(\rho w(z))^{\frac{2}{3}}$, and the vertical integral is evaluated numerically. This procedure, dependent on mean drop radius, is only a crude approximation to radiative transfer in fogs (see Korb and Zdunkowski (1970) for detailed radiative transfer calculations in fog). It provides only a roughly quantitative simulation of the alteration of the vertical distribution of net radiation by fog and the accompanying radiative cooling of the fog. It has, however, the advantage of imposing no significant computational requirements.

Since the observational program has shown conclusively that radiative cooling is a major factor in the development of most marine fogs occurring off the West Coast, the radiative flux divergence computation in the model was altered to take into account a change from a monodisperse droplet population to a spectrum of droplets (after Barker, 1975). The net changes to the model by this modification were to replace the numerical constant 7.1 in Eq. (10) with the constant 19.5 and to alter the method of evaluating the integral of liquid water in Eq. (5). These modifications are included in the program listing provided in Appendix A.

The net effect of these changes in the model of the absorption cross section of the fog is demonstrated by the advection fog simulations (using the new prognostic equations for turbulent energy) presented in Figures 1 and 2. The simulation in Figure 1 uses the former absorption cross section dependent on mean radius, while Figure 2 shows a simulation (of the same initial conditions) using the new formulation. Both fogs are formed over an abrupt decrease

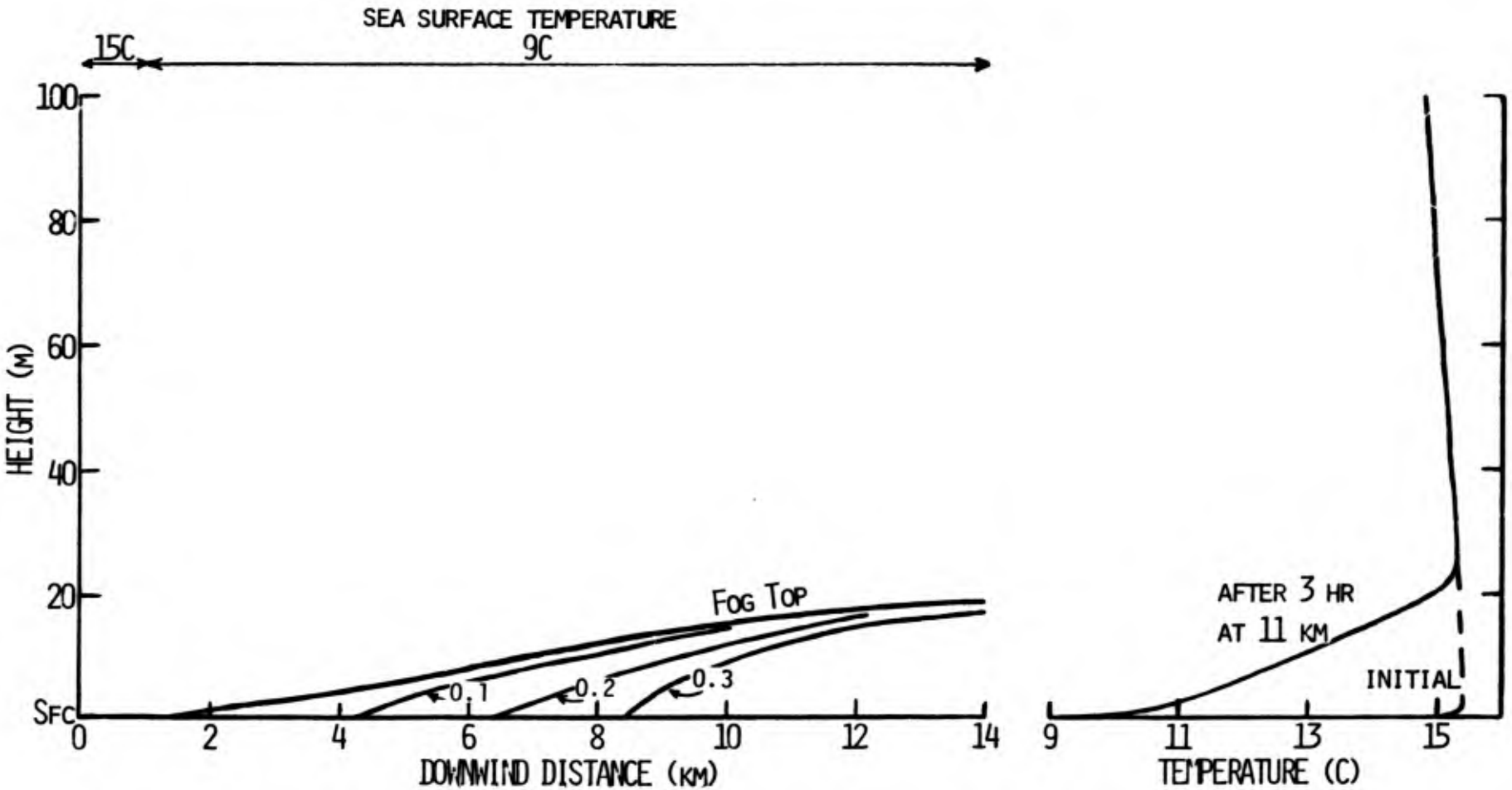

FIGURE 1: CONTOURS OF LWC (G M^{-3}) AND THE VERTICAL TEMPERATURE PROFILE FOR AN ADVECTION FOG SIMULATION BY A NUMERICAL MODEL USING PROGNOSTIC EQUATIONS FOR TURBULENT ENERGY AND A RADIATIVE ABSORPTION COEFFICIENT DEPENDENT ON A MONODISPERSE DROPLET POPULATION.

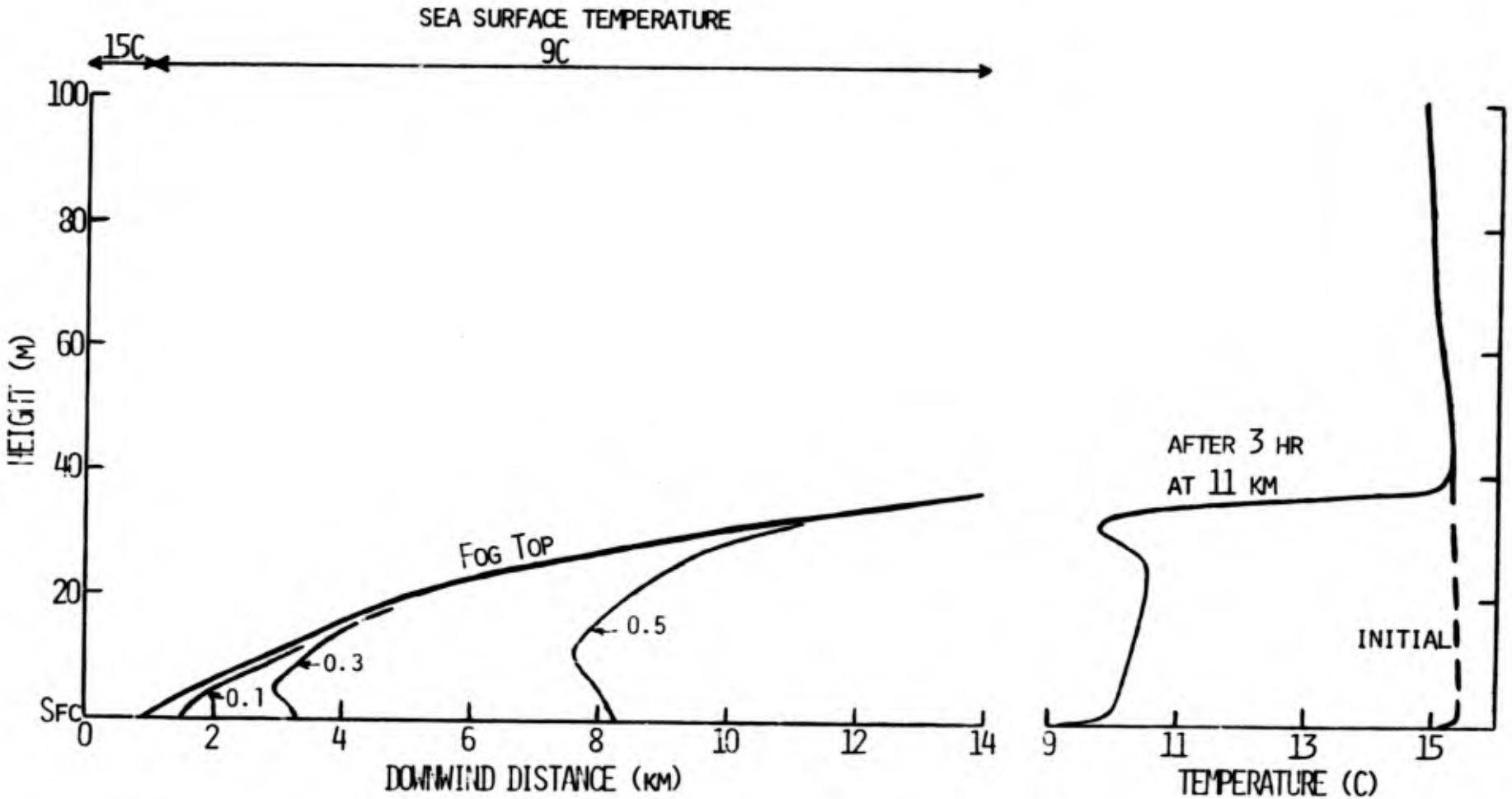

FIGURE 2: CONTOURS OF LWC (G M^{-3}) AND THE VERTICAL TEMPERATURE PROFILE FOR AN ADVECTION FOG SIMULATION BY THE 1976 CALSPAN MODEL USING PROGNOSTIC EQUATIONS FOR TURBULENT ENERGY AND A RADIATIVE ABSORPTION COEFFICIENT DEPENDENT ON A SPECTRUM OF DROPLETS.

in sea surface temperature to 6°C colder than upwind conditions. (The 6°C colder water extends from the 1 km to the 19 km downwind position.) The simulations represent three hours of fog development with winds of 1.6 m sec^{-1} at the 10 m height. Also shown on the figures are the initial upwind and the 11 km downwind vertical temperature profiles.

The effect of the new absorption cross section (compare Figure 2 with Figure 1) is obvious: because of the magnitude of the liquid water initially generated by surface cooling and resultant K_w, radiation becomes more effective in cooling the upper levels of the fog. The upper-level cooling, in turn, intensifies the fog and sharpens the inversion at heights near the fog top. Radiative cooling at upper levels of the fog is reflected by the temperature profile at 11 km. Fog depth at the 11 km downwind position is increased from 16 to 32 m, and maximum LWC is increased from 0.3 to 0.5 g m^{-3}. These results are viewed as particularly important since data collected on all field studies at sea, as well as on land (Mack and Pilié, 1973), indicate that the inversion is raised above the surface when fog thickening reaches 30 to 40 meters

In summary, the general characteristics of the fog in Figure 2 (compared to Figure 1) more closely approximate those observed in shallow fogs off the West Coast. However, the sea surface temperature gradient required to form fog and the resultant LWC are a factor of 2-3 greater than those observed at sea. The simulation shown in Figure 2 suggests that once fog can be realistically triggered (in the model), the handling of radiative flux divergence is improved by the new formulation.

2.2 The Influence of a Warming Sea Surface on the Development of Advection Fog

The Calspan observational studies have shown that sea surface temperature discontinuities of the magnitude required to form fog in the model (e.g., in Figures 1 and 2) are rarely associated with fog formation off the West Coast. Further, a number of fogs have been observed to form or develop

as air advected from cold to warmer water--perhaps as the air advects over the downwind side of a cold water patch after being conditioned over the cold water. These fogs have been thought to be triggered by the vertical mixing initiated by instabilities over the warmer water (Mack et al., 1973).

In an attempt to model such a situation with the Calspan advection fog model, cold water patches have been simulated by advecting air first over abruptly colder water (i.e., 6°C colder than upwind as in Figures 1 and 2) and then over warmer water. In Figure 3 a numerical simulation of advection fog is presented in which air is advected a distance of 3 km over water 6°C colder than upwind and then an additional 10 km over water only 4°C colder than the upwind boundary conditions.

The effect of the warmer water is immediately obvious when comparing Figure 3 with Figure 2. Fog depth increased dramatically as the air advected from the 3 km position to warmer water at the 4 km position. Once fog depth and LWC had increased such that the fog was optically opaque to long wave radiation* (at the 4 km position), the fog began to radiate as a blackbody. Radiative cooling at upper levels produced a LWC increase near fog top. With distance downwind, the combined effects of cooling at fog top and warming at the sea surface resulted in the turbulent mixing of the fog to much greater depths. At the 12 km position, fog top was well above 50 m; and the maximum in LWC was lifted from the surface to the upper two-thirds of the fog.

This is also viewed as an important improvement in the advection fog model. In measurements made at Vandenberg AFB (Rogers et al., 1972) within 1 km of the coast, maximum liquid water contents were consistently found at the upper levels of advection fog.

---

*Previous measurements of radiative transmissivity is shallow radiation fogs on land (Mack and Pilié, 1973) suggest that for a fog to be optically opaque to long wave radiation (and, hence, to radiate as a black body), it must have an optical density equivalent to an integrated liquid water (per square meter over the entire fog depth) in excess of ~3.0 grams.

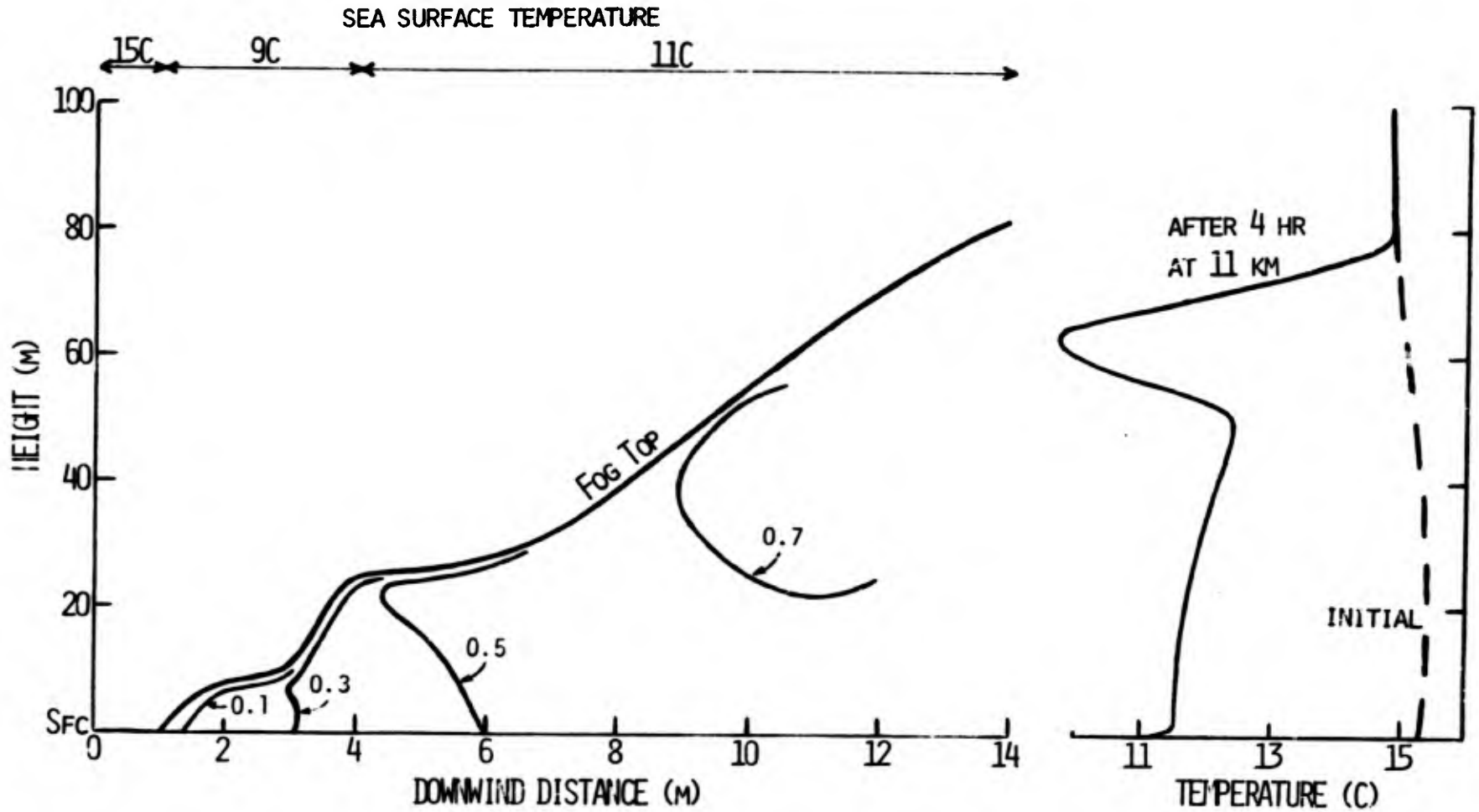

FIGURE 3: CONTOURS OF LWC (G M^{-3}) AND THE VERTICAL TEMPERATURE PROFILE FOR A NUMERICAL SIMULATION OF THE VERTICAL DEVELOPMENT OF AN ADVECTION FOG OVER 2C WARMER WATER BY THE 1976 CALSPAN MODEL.

The vertical temperature profile at 11 km shows maximum cooling near fog top and reflects the influence of radiation. It is apparent from this profile that the model does not yet handle vertical mixing (over great depths) properly. In all fogs sampled to date which were deeper than 50 to 60 m, the observed temperature profile indicated an adiabatic or superadiabatic lapse within the lowest few meters and isothermal to wet adiabatic conditions from that point up to within ~20-30 m of fog top where the inversion begins. It is apparent from Figure 3 that the extreme instability between 50 and 60 m would produce sustained vertical motions. Incorporating the effects of wet adiabatic expansion accompanying such motion would, we believe, accurately reproduce the observed temperature structure in fog.

Carrying this type of numerical experimentation one step further, a simulation is presented in Figure 4 in which, after initial advection over 6°C colder water (as previously done to initiate fog), the air is advected over a sea surface which gradually warmed to within 1°C of the initial upwind boundary conditions. The effect is obvious--fog depth immediately grew beyond 100 m, and fog top ultimately leveled off at a height of 200 m at the 11 km position. In this situation, radiative cooling at fog top is apparently distributed through a deeper layer due to the instabilities and mixing brought about by the much warmer sea surface.

In summary, these simulations of fog formation over and downwind of cold water patches begin to approximate situations previously observed at sea off the coasts of both Nova Scotia and California. The simulations depicted in Figures 3 and 4 closely resemble the fog situation of 4-5 August 1975 off the coast of Nova Scotia reported by Mack and Katz (1976) in Part 1 of this report. The turbulent exchange coefficients computed from predicted values of turbulent energy combined with an increased contribution by radiative influences appear to be much more realistic in simulating development of marine advection fog, particularly over a warming sea surface. However, the magnitude of the sea surface temperature gradient required to trigger fog and the magnitude of resultant liquid water contents remain as principal areas of disagreement between the model and the available observations.

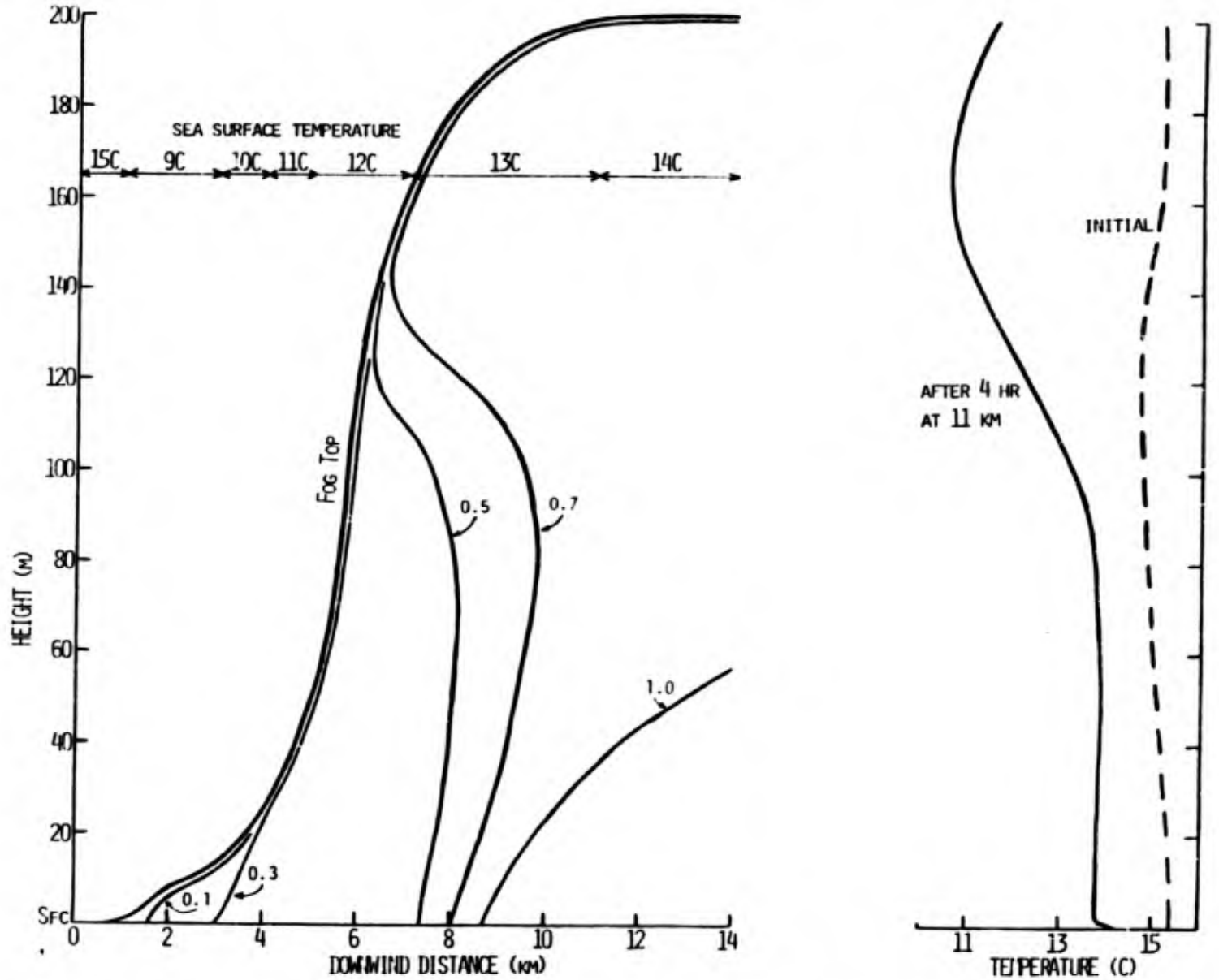

FIGURE 4: CONTOURS OF LWC (G M^{-3}) AND THE VERTICAL TEMPERATURE PROFILE FOR A NUMERICAL SIMULATION OF THE VERTICAL DEVELOPMENT OF AN ADVECTION FOG OVER 5C WARMER WATER BY THE 1976 CALSPAN MODEL.

Section 3

COMPARISON OF A NUMERICAL SIMULATION OF ADVECTION FOG WITH A FOG EVENT OBSERVED OFF THE COAST OF NOVA SCOTIA

During the August 1975 marine fog cruise off the coast of Nova Scotia (Task 1 of this program), several fogs were observed in which formation was attributed to advection of air over cold water and turbulent heat exchange with the sea surface (Mack and Katz, 1976). These observations provide a good reference with which to validate the performance of the 1975 Calspan Advection Fog Model and the effects of the changes incorporated into the model under this program.

3.1 Observations of a Marine Advection Fog

During the late evening of 2 August 1975, a fog was encountered in an area ~50 km offshore near Halifax, Nova Scotia. The fog was quite shallow, with fog top generally at or below the 20 m height. Only in the centermost portion of the fog did fog top reach above the 27 m level, and there only momentarily. Visually, the fog appeared (from the 20 m vantage point) as sketched in Figure 5. Fog depth increased gradually from the edges toward the center of the fog, and fog top was very ragged--unlike the smooth, regular appearance of fogs formed beneath and capped by inversion layers.

The microphysical features of the fog are difficult to assess because sampling instrumentation was located at a height of 20 m (i.e., near fog top). Thus, the measurements of fog microphysics for the fog may be representative of fog top only. Briefly summarizing, mean drop radii of about 5 μm and maximum drop sizes of ~17 μm were characteristic of the fog. Droplet concentration varied from about 30 to 110 cm^{-3}, and liquid water content ranged from ~0.03 to ~0.20 g m^{-3}. Minimum observed visibility was <100 m.

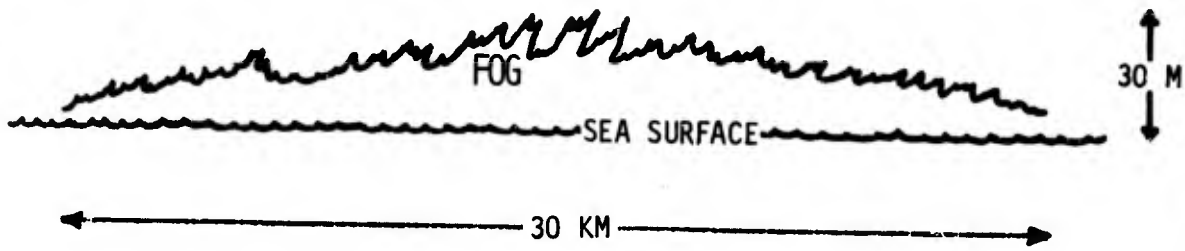

FIGURE 5: SKETCH OF THE VERTICAL PROFILE OF THE FOG OF 1915-0040, 2-3 AUGUST 1975.

In Figures 6 and 7, the ship's track has been reproduced and an attempt has been made to delineate boundaries of the fog by isopleths of visibility (Figure 6) and to draw isotherm contours for the sea surface (Figure 7). Visibility isopleths are labeled in meters, and the 1000 m visibility level is represented by the scalloped line. Note that the contours of visibility follow the general pattern of the sea surface isotherms and that the fog was located over and just downwind of the coldest water in the vicinity. The best wind information indicates that during the period of observation of the fog, winds shifted gradually from southerly at 1800 EDT to SE (~140°) by 2200 EDT. Unfortunately, sea surface temperature data are not available from the upwind quadrant, and thus it is not possible to demonstrate conclusively that this fog formed as a direct result of cooling from below.

Some insight into the mechanism responsible for this fog may be deduced from analyses of the vertical temperature profiles and surface-level humidity data obtained in the vicinity. In Figure 8 selected vertical temperature profiles (surface to 27.5 m) are shown for the areas outside the western, eastern, and southern boundaries (5000 m visibility isopleth) of the fog and for the center region of the fog. Approximate upwind conditions may be represented by the two profiles (shown dashed) obtained outside the southern boundary of the fog before and after (1630 and 0050 EDT) encountering the fog. These two profiles indicate that upwind conditions remained relatively unchanged through the period. Note that all profiles exhibited

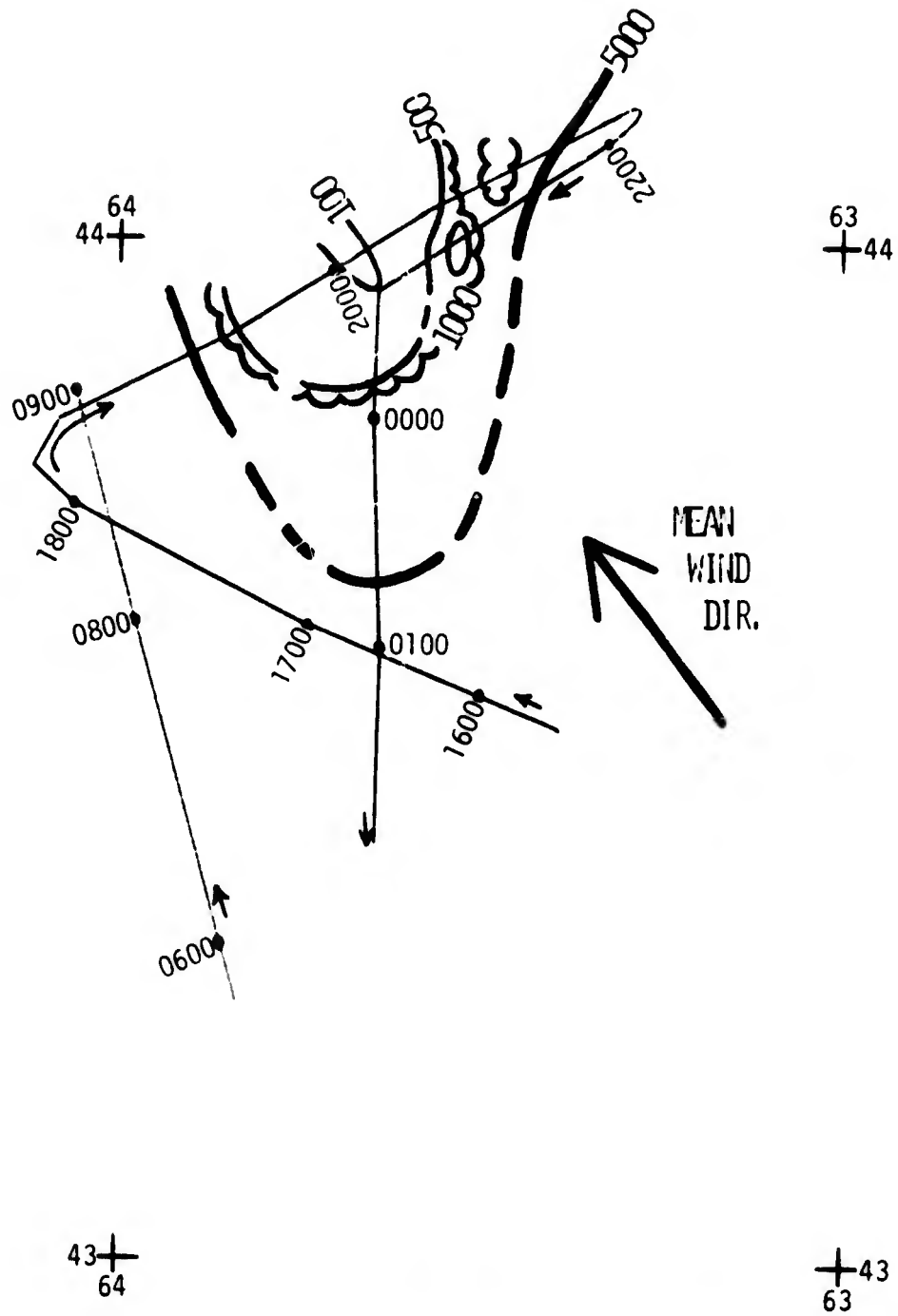

FIGURE 6: CONTOURS OF VISIBILITY (M) FOR THE FOG OF 1915-0040 EDT, 2-3 AUGUST 1975.

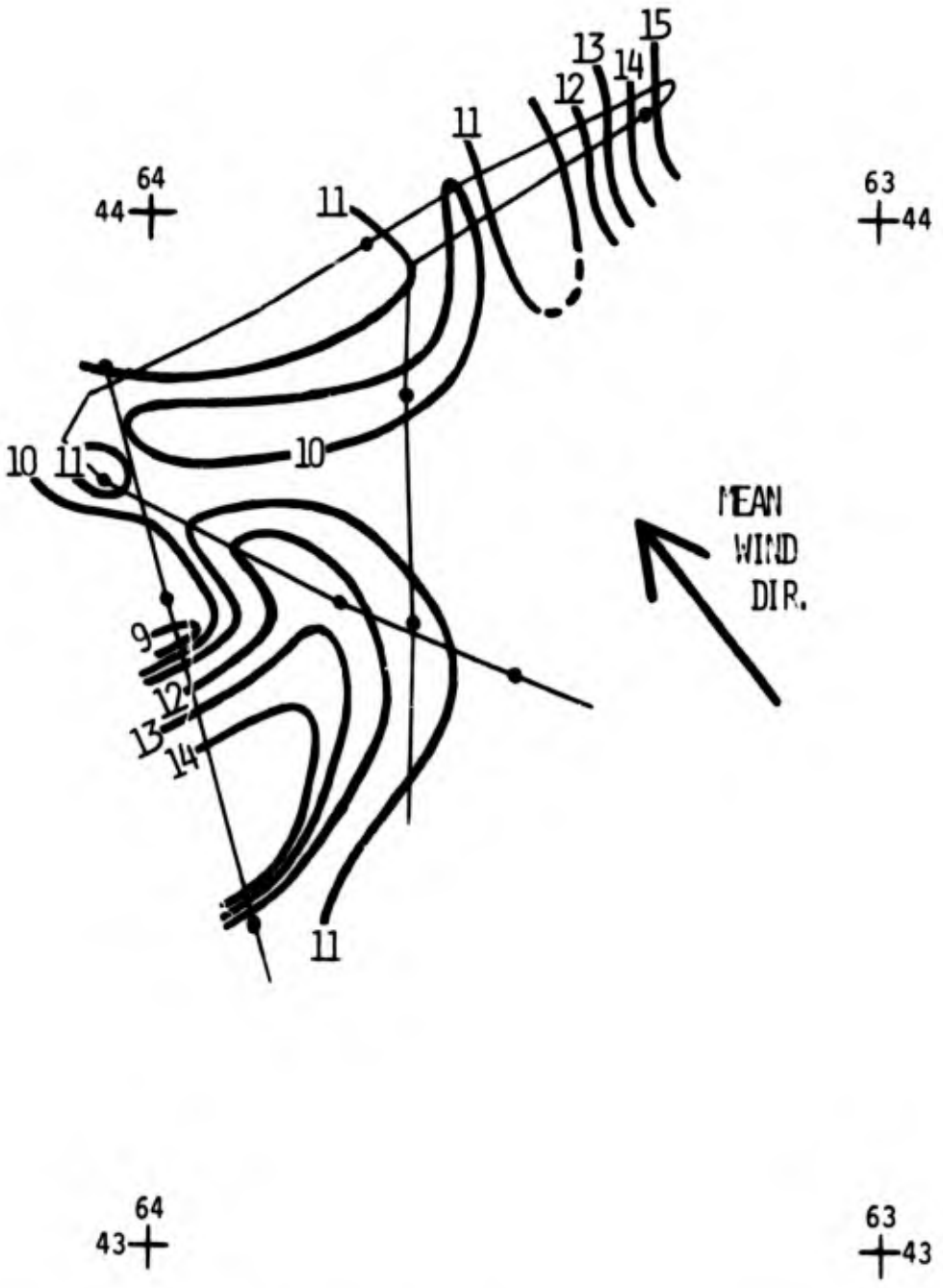

FIGURE 7: SEA SURFACE ISOTHERM (C) CHART FOR THE FOG OF 1915-0040, 2-3 AUGUST 1975.

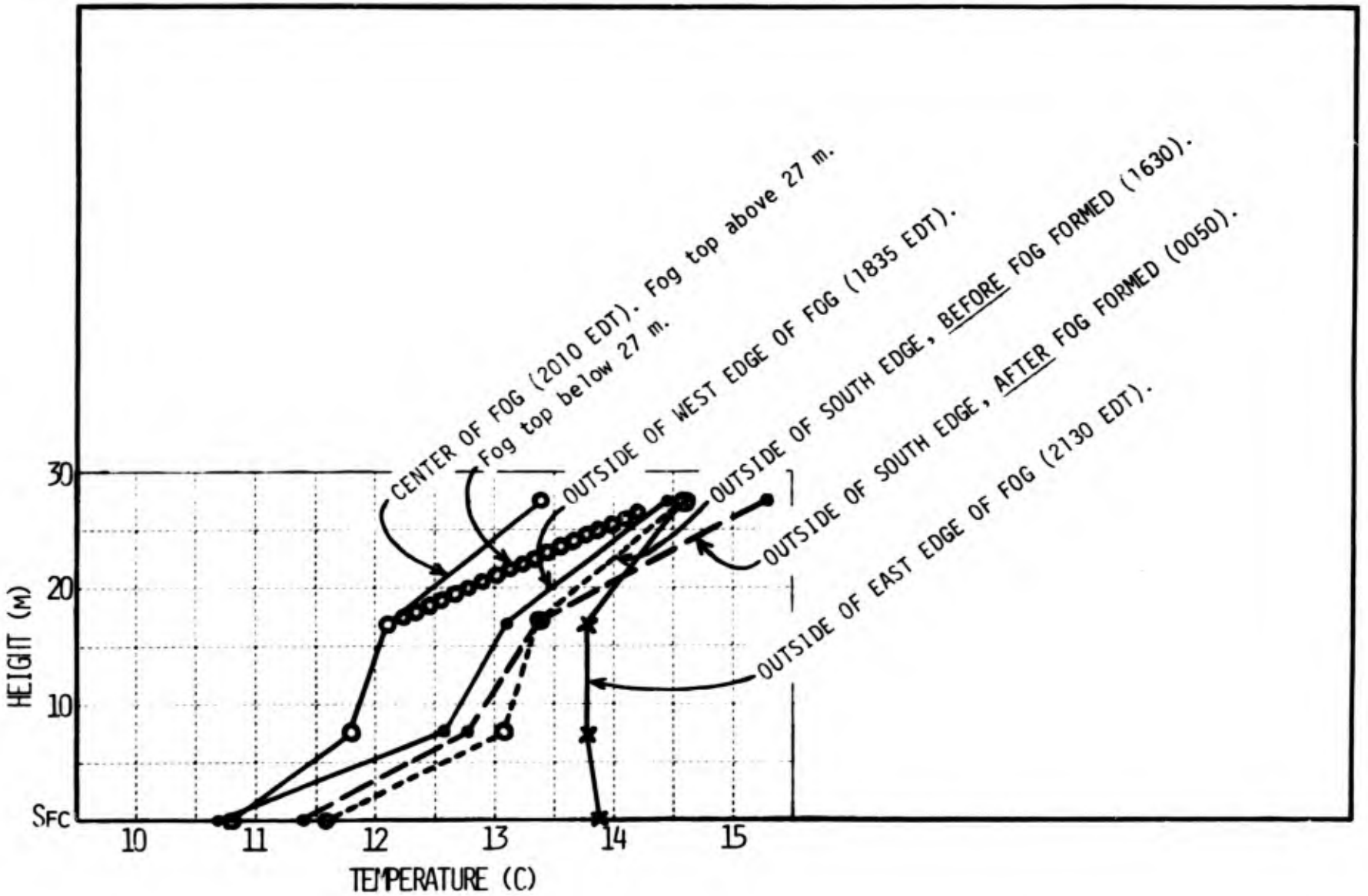

FIGURE 8: SELECTED VERTICAL TEMPERATURE PROFILES IN AND AROUND THE FOG OF 2-3 AUGUST 1975.

an inverted lapse down to the surface and that the absolute values of air temperature were similar at all points outside the fog except for the near-surface level at the eastern edge of the fog. (Vertical soundings obtained at 1730 and 2030 EDT by Gathman (1976) show that the inverted lapse extended up to ~200 m.) From Figure 7, it can be seen that advection of air nearly parallel to sea surface isotherms accounts for the small change (from upwind conditions) in air temperature along the western edge of the fog and that advection from substantially warmer water can account for the warmer air temperatures along the eastern edge of the fog. The temperature profile at the eastern boundary may be more representative of far upwind conditions; i.e., perhaps 50 km upwind.

The sea surface temperature immediately downwind of the fog was the coldest (i.e., ~9.5°C) observed along ship's track in the area and may have been even colder in the area farther upwind (not traversed). It can be seen from Figure 8 that within the fog the inverted lapse was maintained, but that after advection over the cold water lower level air temperatures were colder by ~1.5°C than upwind conditions. At levels above fog top, air temperatures were nearly the same as those measured at upwind locations--indicating a cooling mechanism confined to the lowest tens of meters.

It appears that a sea surface temperature gradient--from ~11.5°C in the general upwind area to ~9.5°C under the leading edge of the fog--was responsible for cooling the boundary layer (below ~25 m) by ~1.5°C. Upwind of the fog, measured relative humidity was approximately 90% (89-94% depending on the instrumentation one wishes to believe). At these relative humidities, cooling of the air by 1.5°C is more than sufficient to produce saturation (assuming no water vapor losses to the cold sea surface) and account for the fog. The ragged structure of the fog top and the shallow depth of the fog are, in themselves, indicative of boundary exchange processes, driven by surface-level influences.

3.2 Numerical Simulations of Fog Formed by Turbulent Heat Exchange with a Cold Sea Surface and Comparison with Observations

A numerical model which allows turbulent fluxes of both heat and moisture to the underlying ocean surface was developed previously at Calspan (Rogers et al., 1975) and was the object of minor modifications under the current contract. In a simulation with this model, made prior to the August 1975 Nova Scotia cruise, fog was formed starting from initial conditions consisting of an isothermal temperature profile and a relative humidity of 98%. The air was advected over a 4°C discontinuity in water temperature; and after four hours, a steady-state fog extended from the temperature discontinuity to 24 km downwind. At 10 km the fog was 5 m deep and had a liquid water content of 0.09 g m^{-3}; cooling was restricted to below 15 m with the air immediately next to the ocean surface experiencing a temperature decrease of 3.5°C. The results of this numerical simulation are plotted at the top of Figure 9.

In order to show the effects of the changes incorporated into the 1975 version of the model, simulations of marine advection fog (starting with the same initial conditions as above, except that of sea surface temperature) using two versions of the 1976 model are shown at the middle and bottom of Figure 9. These two versions of the model represent the two evolutionary steps in the modification of the model achieved under this contract.

The fog depicted in the middle of Figure 9 was formed with the 1975 version of the model in which the prognostic equations for turbulent energy had been incorporated. In this simulation, fog was formed, starting with an isothermal temperature profile and a RH of 99%, by advecting the air over water abruptly 5°C colder than upwind. After three hours, a steady-state fog extended to 18 km downwind. At 10 km, the fog was 10 m deep, with a maximum LWC of 0.18 g m^{-3}; cooling was restricted to the lowest 20 m and was greatest next to the surface.

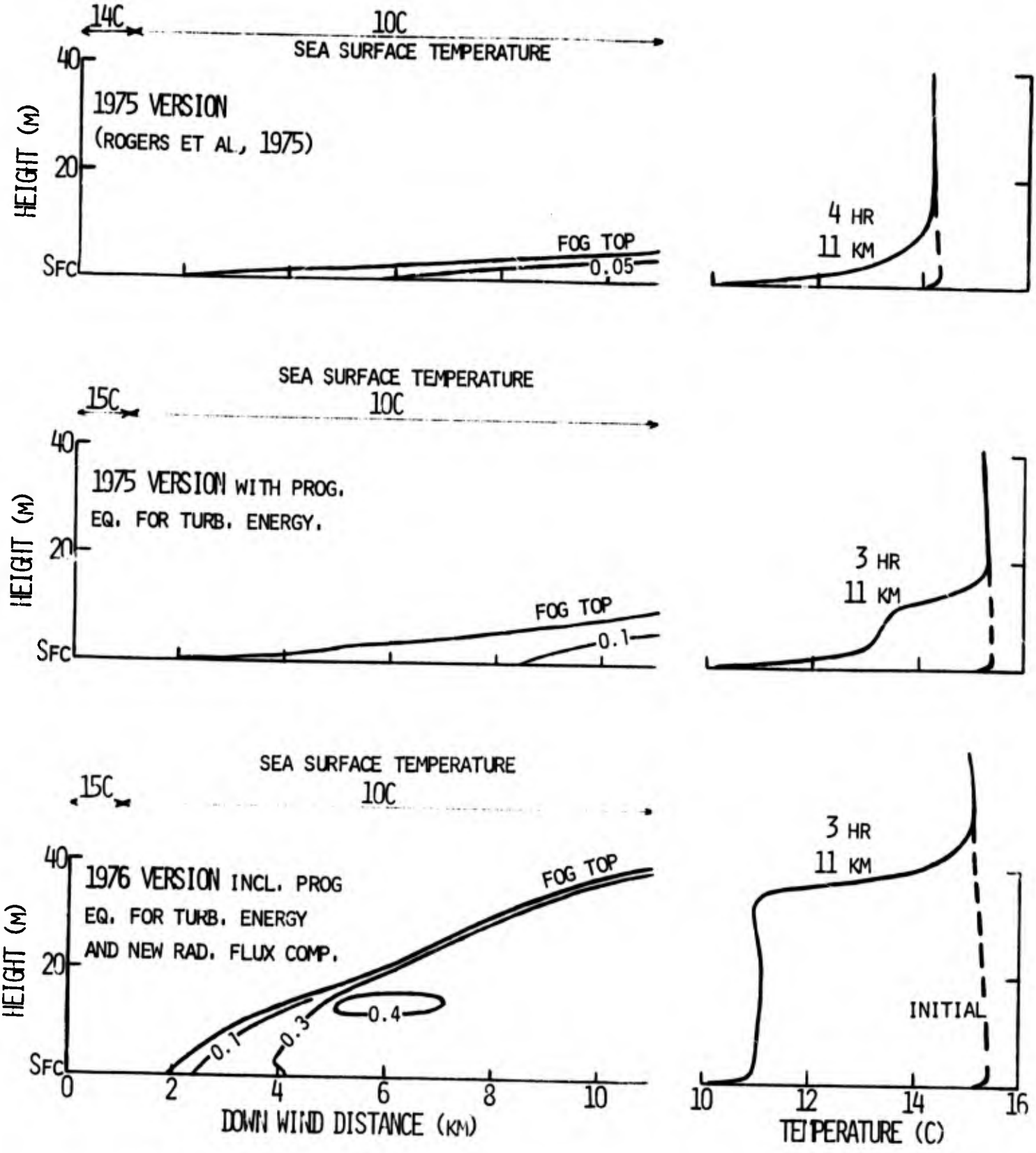

FIGURE 9: RESULTS OF NUMERICAL SIMULATION OF MARINE ADVECTION FOG USING THREE VERSIONS OF THE CALSPAN ADVECTION FOG MODEL.

The fog shown at the bottom of Figure 9 was formed with the 1976 version of the model in which both the new parameterization of radiation and the prognostic equations for turbulent energy had been incorporated. (The Fortran listing for this model is provided in Appendix A.) Again, using the same initial conditions as above, a steady-state fog extended to 18 km downwind after three hours. At 10 km fog depth was 35 m, and maximum LWC was 0.4 g m^{-3}. In this fog while cooling was again restricted to the fog layer, substantial cooling occurred throughout the layer. The cooling observed in the upper levels of the fog, as demonstrated by the temperature profile, was a result of the new parameterization of radiation.

Additional parameters from the fog simulated with the 1975 and 1976 versions of the model are compared in Table 1 with those observed in the fog of 2-3 August 1975. The correspondence between observed and predicted (1976 version of the model) values of the various parameters is striking. Agreement of any of the individual parameters would be striking, but the close agreement of all seven parameters clearly establishes the 1976 model's value for simulation of shallow fog formed by cooling from below.

One parameter which did not correlate well between the 1975 version of the model and the observations was that of fog depth. The shallow fog predicted by the model was a direct result of the previous turbulence modeling, a factor which also influenced the distribution of cooling in the vertical. Within the numerical simulation, eddy transfer was suppressed in the low levels in order to form fog. As a result of this turbulence suppression, strong eddy transport could not exist at higher levels; therefore, cooling was concentrated below 10 m, and fog top was limited to about 5 m. The turbulence modeling in the 1975 version of the numerical model was hampered by the following problem: if turbulence was kept small enough to form fog by cooling at the surface, then fog could not grow to great depths. On the other hand, if turbulence was permitted to be large enough so that fog could grow to greater depths, then fog did not form initially.

Table 1: COMPARISON OF MODEL PARAMETERS WITH OBSERVATIONS

Parameter	Observed	1976 Model	1975 Model
Initial Temp Profile	Isothermal 14C	Isothermal 15C	Isothermal 14C
RH	89-94%	99%	98%
Sea Surface Temp Diff.	2-4C	5C	4C
Depth of Cooled Layer	<27 m	<35 m	<15 m
Fog Depth	~30 m	35 m	5 m
LWC (max)	0.2 g m^{-3}	0.4	0.09 g m^{-3}
Advection Distance from Edge to Fog Center	15 km	10 km	10 km
Wind Speed @ 10 m	5 m sec^{-1}	1.7 m sec^{-1}	1.7 m sec^{-1}

The current modeling effort therefore was directed toward improving the turbulence modeling so that large turbulence values present at higher levels could overlie smaller turbulence values, apparently necessary near the surface--thus, fog would not only form by cooling at the surface but would also grow to greater depths. It appears that these efforts have been at least partially successful as demonstrated by the close correspondence between the observed and simulated advection fogs.

REFERENCES

Barker, E.H., 1975: A Maritime Boundary Layer Model for the Prediction of Fog, Tech. Paper No. 4-75, Environmental Prediction Research Facility, Naval Postgraduate School, Monterey, CA 93940.

Gathman, S.G., 1976: Boundary Layer Measurements of Temperature, Water Vapor and Pressure During the 1975 Fog Cruise of the USNS HAYES, Compilation of Data from the 1975 USNS HAYES Fog Cruise, Naval Research Laboratory Rept. No. 7_ _ _, (in press).

Goody, R.M., 1964: Atmospheric Radiation. Oxford University Press, 436 pp.

Korb, G., and W. Zdunkowski, 1970: Distribution of Radiative Energy in Ground Fog. Tellus, 22, 298-320.

Mack, E.J., W.J. Eadie, C.W. Rogers, W.C. Kocmond, and R.J. Pilié, 1972: A Field Investigation and Numerical Simulation of Coastal Fog, Calspan Report No. CJ-5055-M-1, Calspan Corporation, Buffalo, N.Y. 14221.

Mack, E.J., R.J. Pilié, and W.C. Kocmond, 1973: An Investigation of the Microphysical and Micrometeorological Properties of Sea Fog, Project SEA FOG: First Annual Summary Report, Report No. CJ-5237-M-1, Calspan Corporation, Buffalo, N.Y. 14221.

Mack, E.J. and R.J. Pilié, 1973: The Microstructure of Radiation Fog at Travis AFB, Rept. No. CJ-5076-M-2, Calspan Corporation, Buffalo, N.Y. 14221.

Mack, E.J., U. Katz, C.W. Rogers, and R.J. Pilié, 1974: The Microstructure of California Coastal Stratus and Fog at Sea, Project SEA FOG: Second Annual Summary Report, Calspan Report No. CJ-5404-M-1, Calspan Corporation, Buffalo, N.Y. 14221.

Mack, E.J., R.J. Pilié, and U. Katz, 1975: Marine Fog Studies Off the California Coast, Project SEA FOG: Third Annual Summary Report, Calspan Report No. CJ-5067-M-1, Calspan Corporation, Buffalo, N.Y. 14221.

Mack, E.J. and U. Katz, 1976: The Characteristics of Marine Fog Occurring Off the Coast of Nova Scotia, Project SEA FOG: Fourth Annual Summary Report, Part 1, Calspan Rept. No. CJ-5756-M-1, Calspan Corporation, Buffalo, N.Y. 14221.

Pepper, D.W. and S.C. Lee, 1974: Transport Phenomena in Thermally Stratified Boundary Layers, Proc. AIAA/ASME Thermophysics and Heat Transfer Conference, July 15-17, 1974, Boston, Mass.

Rogers, C.W., W.J. Eadie, U. Katz and W.C. Kocmond, 1975: A Numerical Model of Advection Fog, Project FOG DROPS V, NASA CR-2633, National Aeronautics and Space Admin., Wash., D.C. 20546, 79 pp., $4.75.

Sutton, O.G., 1953: Micrometeorology, New York, McGraw-Hill, 333 pp.

Zdunkowski, W.G., and B.C. Nielsen, 1969: A Preliminary Prediction Analysis of Radiation Fog, Pure and Appl. Geophys., 75, 278-299.

APPENDIX A

FORTRAN LISTING OF COMPUTER PROGRAM WITH COMMENT CARDS

FOR

THE CALSPAN TWO-DIMENSIONAL ADVECTION FOG MODEL

JUNE 1976

CALSPAN CORPORATION
BUFFALO, NEW YORK 14221

```
C
C
C     TWO-DIMENSIONAL ADVECTION FOG MODEL
C     STEADY STATE MODEL
C
C     CALSPAN CORP.  1976
C
C
      REAL*8 PT,EPT,FPT,DPT,AT,CT,BT
      REAL*4 KA,INT,KW,L,LM,LMAX,KM,LMM
      COMMON PT(40,60),EPT(60),FPT(60),DPT,AT,CT,BT,
     8     WINT(40,60),R(40,60),W(40,60),U(40,60),T(40,60),KA(40,60),
     7KM(40,60),LM(60),LMM(60),Q(40,60),EQ(60),FQ(60),
     1        INT(40,60),CPT(40,60),HC(40,60),X(40),DX(40),DTEM(40),
     2        P(60),ZA(60),DZA(60),                    ER(60),FR(60),EW(60),
     3        FW(60),EU(60),FU(60),Z(60),DZ(60),PR(60),L,DEN,CP,G,RA,RW,
     4        SIGMA,TIME,DT,TIM,UF,RF,KW,ZO,CV,UI,DTEMI,ZAK,XAI,DELX,CC,
     5        CH,CI,CK,CL,CR,CS,UU,FV(60),EV(60),V(40,60),     F,
     6        KE,KN,IE,IN,IL,IR,ISED,IRAD,IRSFC,IDTEM,ITEML,ITEMR,IP,II
      DIMENSION FMTH(11),FMTT(11)
C
C     PHYSICAL CONSTANTS
C
      L=592.
      DEN=1.23E-3
      CP=.240
      G=980.6
      RA=.0686
      RW=.1102
      SIGMA=1.355E-12
      CV=1.07E+3
      F=1.0E-4
      P(1)=1000.
C
C     DATA INPUT
C
   10 READ(5,1000,END=400) DT,OT,ET,TIM,RF,KW,TP,ZO,DTEMI,UF
      READ(5,1100) IPT,IRR,IW,ISED,IRAD,IRSFC,IU,IDTEM,IP,II,KT,KR,IZ
      READ(5,1200) ZAL,ZAK,XAI,IE,KE,IL,IR,ITEML,ITEMR,DELX
      READ(5,1205) FMTH,FMTT
C
C     DATA LISTING
C
      WRITE(6,2000) DT,OT,ET,TIM,RF,KW,TP,ZO,DTEMI,UF
      WRITE(6,2100) IPT,IRR,IW,ISED,IRAD,IRSFC,IU,IDTEM,IP,II,KT,KR,IZ
      WRITE(6,2200) ZAL,ZAK,XAI,IE,KE,IL,IR,ITEML,ITEMR,DELX
C
C     WORKING CONSTANT DEFINITION
C
      LMAX=.015*UF/F
      CC=.622*(L**2)/(CP*RA)
      CR=KW*RF*SIGMA/(CP*DEN**.333)
      CI=KW*DEN**.667
      CH=(L**2)/RW
      CK=.4*UF
      CS=G/4.186E+7
      IN=IE-1
      KN=KE-1
C
C     VERTICAL GRID SPECIFICATION
C
```

```
      ZA(1)=0.0
      ZA(2)=ZAL
      DZA(2)=ZAL
      DO 20 K=3,KE
      ZA(K)=(1.+ZAK)*ZA(K-1)
   20 DZA(K)=ZAK*ZA(K-1)
      DO 25 K=2,KE
      Z(K)=(ZA(K)+ZA(K-1))/2.
   25 CONTINUE
C
C     HORIZONTAL GRID SPECIFICATION
C
      DO 30 I=IL,IR
   30 X(I)=(I-IL)*DELX
      I1=IR+1
      DO 31 I=I1,IE
   31 X(I)=X(I-1)+XAI*(X(I-1)-X(I-2))
      IF(IL .EQ. 1) GO TO 33
      I1=IL-1
      DO 32 I2=1,I1
      I=I1-I2+1
   32 X(I)=X(I+1)-XAI*(X(I+2)-X(I+1))
   33 DO 35 I=2,IE
   35 DX(I)=X(I)-X(I-1)
C
C
C     VARIABLE INITIALIZATION
C
C
      READ(5,1300) RI,PTI
      WRITE(6,2300) RI,PTI
      TP=TP+.16
      PTI=PTI+.16
      W(1,1)=0.0
C
C     A-UNIFROM WITH HEIGHT
C
      DO 40 I=1,IE
      DO 40 K=1,KE
      W(I,K)=0.0
      R(I,K)=RI
       PT(I,K)=PTI
      IF(I .EQ. 1) P(K)=1000.*EXP(-G*ZA(K)/(4.186E+7*RA*TP))
C
C     B-ISOTHERMAL
C
      IF(IPT .EQ. -1) PT(I,K)=TP*((1000./P(K))**.286)
C
C     D-QUASI-ADIABATIC VELOCITY PROFILES
C
      IF(IU.EQ. 0) U(I,K)=2.5*UF*ALOG((ZA(K)+ZO)/ZO)
      IF(IU .EQ. 0) V(I,K)=-2.5*UF*2.8*ZA(K)/ZA(KE)
      IF(IU .EQ. 0) Q(I,K)=4.*(UF**2)*(1.-ZA(K)/ZA(KE))**2
C
   40 CONTINUE
C
C     INITIALIZE 2-D SIMULATION  FROM 1-D SIMULATION
C     III=2 INITIALIZES UPWIND BOUNDARY  III=1 INITIALIZES REST OF DOMAIN
C
      DO 500  III=1,1
      IF(IU .EQ. 1) READ(5,4000) (U(1,K),K=1,KE)
```

```
      IF(IU .EQ. 1) READ(5,4000) (V(1,K),K=1,KE)
C
C      KT AND KR PERMIT NON-UNIFORM INITIALIZATION OF 1-DIMENSIONAL
C     SIMULATIONS FROM KT AND KR LEVELS TO TOP OF THE MODEL
C
      IF(IPT .EQ. 1) READ(5,5000) (PT(1,K),K=KT,KE)
      IF(IRR .EQ. 1) READ(5,4000) (R(1,K),K=KR,KE)
      IF(IW .EQ. 1) READ(5,4000) (W(1,K),K=KR,KE)
      IF(IU .EQ. 1) READ(5,4000) (Q(1,K),K=1,KE)
      IF(IU .EQ. 1) WRITE(6,2500) (U(1,K),K=1,KE)
      IF(IU .EQ. 1) WRITE(6,2500) (V(1,K),K=1,KE)
      IF(IPT .EQ. 1) WRITE(6,2400) (PT(1,K),K=1,KE)
      IF(IRR .EQ. 1) WRITE(6,2500) (R(1,K),K=1,KE)
      IF(IW .EQ. 1) WRITE(6,2500) (W(1,K),K=1,KE)
      IF(IU .EQ. 1) WRITE(6,2500) (Q(1,K),K=1,KE)
C
      IF(IPT .EQ. 1) GO TO 45
      GO TO 60
C
C     PT AND W FROM VARIABLE LIST
C
   45 CONTINUE
C
C     INITIALIZE ONLY THE UPWIND COLUMN
C
      IF(III .EQ. 2) GO TO 501
C
C     INITIALIZATION ALL COLUMNS
C
      DO 50 I=2,IE
      DO 50 K=1,KE
      U(I,K)=U(1,K)
      V(I,K)=V(1,K)
      PT(I,K)=PT(1,K)
      R(I,K)=R(1,K)
      Q(I,K)=Q(1,K)
   50 W(I,K)=W(1,K)
   60 CONTINUE
C
C     INITIALIZATION,EXCHANGE COEFFICIENT, INTEGRATED LIQUID WATER,AND
C     SPECIFIC HEAT OF MOIST AIR
C
  501 CONTINUE
      CL=14.*G*.16/PT(1,1)
      WINT(1,1)=0.
      INT(1,1)=0.0
      T(1,1)=PT(1,1)
      DO 80 K=2,KE
      WINT(1,K)=0.
      LM(K)=.4*(Z(K)+ZO)/(1.+.4*Z(K)/LMAX)
      DWZ=SQRT((U(1,K)-U(1,K-1))**2+(V(1,K)-V(1,K-1))**2)/DZA(K)
      PR(K)=(1000./P(K))**.286
      IF(K .EQ. KE) GO TO 64
      DZ(K)=.5*DZA(K)*(DZA(K)+DZA(K+1))
   64 T(1,K)=PT(1,K)/PR(K)
      IF(W(1,K) .GT. 0.0) GO TO 65
      CPT(1,K)=CP
      GO TO 70
   65 CPT(1,K)=CP+CH*RSF(T(1,K),P(K))/(T(1,K)**2)
C
C     INITIALIZATION OF EXCHANGE COEFFICIENTS COVERING NEUTRAL,STABLE AN
```

```
C     UNSTABLE CONDITIONS BETWEEN K=2 AND THE SURFACE
C
   70 IF(K .EQ. 2) GO TO 71
      QM=Q(1,K)
      KM(1,K)=.50*SQRT(QM)*LM(K)
      KA(1,K)=KM(1,K)
      GO TO 80
   71                 KM(1,2)=.16*SQRT(U(1,2)**2+V(1,2)**2)*DZA(2)/(ALOG((Z
     1A(2)+ZO)/ZO)**2)
                      KA(1,2)=KM(1,2)
   80 INT(1,K)=INT(1,K-1)+CI*DZA(K)*W(1,K)**.667
      CPT(1,1)=CPT(1,2)
      KA(1,1)=KA(1,2)
C
      IF(III .EQ. 2) GO TO 502
C     INITIALIZATION ALL COLUMNS
C
      DO 81 I=2,IE
      DO 81 K=1,KE
      IF(K .EQ. 1) W(I,K)=0.0
      T(I,K)=T(1,K)
      CPT(I,K)=CPT(1,K)
      KM(I,K)=KM(1,K)
      KA(I,K)=KA(1,K)
      WINT(I,K)=WINT(1,K)
   81 INT(I,K)=INT(1,K)
  500 CONTINUE
  502 CONTINUE
C
C     INITIALIZATION OF SURFACE TEMPERATURE DIFFERENCE
C
      IF(IDTEM .EQ. -1) GO TO 86
      DO 85 I=1,IN
      IF(IDTEM .EQ. 0) DTEM(I)=0.0
      IF(IDTEM .EQ. 1) DTEM(I)=DTEMI
      IF((IDTEM .EQ. 1) .AND. (I .LT. ITEML)) DTEM(I)=0.0
      IF((IDTEM .EQ. 1) .AND. (I .GT. ITEMR)) DTEM(I)=0.0
   85 CONTINUE
      GO TO 87
   86 READ(5,1400) (DTEM(I),I=2,IN)
      WRITE(6,2400) (DTEM(I),I=2,IN)
      DTEM(1)=0.0
      DTEM(IE)=0.0
C
C     UPPER BOUNDARY CONDITION FOR IMPLICIT INTEGRATION
C
   87 EU(KE)=0.
      EV(KE)=0.
      EPT(KE)=0.0
      ER(KE)=0.0
      EW(KE)=0.0
      EQ(KE)=0.
      FU(KE)=U(1,KE)
      FV(KE)=V(1,KE)
      FPT(KE)=PT(1,KE)
      FR(KE)=R(1,KE)
      FW(KE)=W(1,KE)
      FQ(KE)=Q(1,KE)
C
C     OUTPUT TIME ,END TIME, AND TIME STEP CONTROL
C
```

```
      TIME=0.0
      PRT=DT
   90 IF(TIME .LT. PRT) GO TO 95
      PRT=TIME+DT
      GO TO 200
   95 IF(TIME .GE. ET) GO TO 10
      TIME=TIME+DT
      CALL STEP
      GO TO 90
  200 CONTINUE
C
C
C     OUTPUT
C
C
C
C     EDDY HEAT FLUX OUTPUT
C
  300 WRITE(6,3000)
      DO 311 I=1,IE
      DO 310 K=3,KN
      IF(CPT(I,K) .LE. CP) HC(I,K)=-DEN*CP*((KA(I,K+1)*(PT(I,K+1)-PT(I,K
     1))/(ZA(K+1)-ZA(K)))+(KA(I,K)*(PT(I,K)-PT(I,K-1))/(ZA(K)-ZA(K-1))))
     2*2.1
  310 IF(CPT(I,K) .GT. CP) HC(I,K)=-DEN*CPT(I,K)*(((KA(I,K)+KA(I,K+1))/2
     1.)*((T(I,K+1)-T(I,K-1))/(ZA(K+1)-ZA(K-1))+CS/CPT(I,K)))*4.2
      WINDV2=SQRT(U(I,2)**2+V(I,2)**2)*.07
      IF(CPT(I,2) .LE. CP) HC(I,2)=-DEN*CP*60.*.16*WINDV2*(PT(I,2)-PT(I,
     11))/(ALOG((ZA(2)+ZO)/ZO)**2)
      IF(CPT(I,2) .GT. CP) HC(I,2)=-DEN*CPT(I,2)*60.*.16*WINDV2*(T(I,2)-
     1T(I,1)+CS*ZA(2)/CPT(I,2))/(ALOG((ZA(2)+ZO)/ZO)**2)
      HC(I,1)=HC(I,2)
      HC(I,KE)=HC(I,KN)
  311 CONTINUE
      CALL PRNT(HC,FMTH)
C
C     LOCAL FRICTION VELOCITY OUTPUT
C
      WRITE(6,3008)
      DO 313 I=1,IE
      DO 312 K=3,KN
      FLUX=(KM(I,K+1)*SQRT((U(I,K+1)-U(I,K))**2+(V(I,K+1)-V(I,K))**2)/DZ
     1A(K+1) +KM(I,K)*SQRT((U(I,K)-U(I,K-1))**2+(V(I,K)-V(I,K-1))**2)/DZ
     2A(K))/2.
      IF(FLUX .GT. 0.) HC(I,K)=SQRT(FLUX)
  312 CONTINUE
      WINDV2=SQRT(U(I,2)**2+V(I,2)**2)
      HC(I,2)=.4*WINDV2/ALOG((ZA(2)+ZO)/ZO)
      HC(I,1)=HC(I,2)
  313 HC(I,KE)=HC(I,KN)
      CALL PRNT(HC,FMTH)
C
C
C
C
C     WIND OUTPUT
C
      WRITE(6,3009)
      DO 314 I=1,IE
      DO 314 K=1,KE
  314 HC(I,K)=1.0E-2*U(I,K)
```

```
      CALL PRNT(HC,FMTH)
      WRITE(6,3010)
      DO 316 I=1,IE
      DO 316 K=1,KE
  316 HC(I,K)=1.0E-2*V(I,K)
      CALL PRNT(HC,FMTH)
      WRITE(7,4000) (U(IZ,K),K=1,KE)
      WRITE(7,4000) (V(IZ,K),K=1,KE)
C
C     TEMPERATURE OUTPUT
C
      WRITE(6,3100)
      CALL PRNT(T,FMTT)
      WRITE(7,5000) (PT(IZ,K),K=1,KE)
C
C     MIXING RATIO OUTPUT
C
      WRITE(6,3200)
      CALL PRNT(R,FMTH)
      WRITE(7,4000) (R(IZ,K),K=1,KE)
C
C     LIQUID WATER CONTENT OUTPUT
C
      WRITE(6,3300)
      DO 315 I=1,IE
      DO 315 K=1,KE
  315 HC(I,K)=DEN*W(I,K)*1.0E+6
      CALL PRNT(HC,FMTH)
      WRITE(7,4000) (W(IZ,K),K=1,KE)
C
C     DEW POINT DEPRESSION OUTPUT
C
      WRITE(6,3400)
      DO 320 I=1,IE
      DO 320 K=1,KE
C
C     DEW POINT DEPRESSION COMPUTATION
C
      E=P(K)*R(I,K)/(.62465+R(I,K))
      T1=T(I,K)
      DO 318 M=1,3
      RS=RSF(T1,P(K))
      ES=P(K)*RS/(.62465+RS)
      EE=E/ES
  318 T1=T1+(T1-35.86)*ALOG(EE)/17.26939
  320 HC(I,K)=T(I,K)-T1
      CALL PRNT(HC,FMTH)
C
C     TURBULENT ENERGY OUTPUT
C
      WRITE(6,3410)
      CALL PRNT(Q,FMTH)
      WRITE(7,4000) (Q(IZ,K),K=1,KE)
C
C     TURBULENT EXCHANGE COEFFICIENT OUTPUT
C
      WRITE(6,3500)
      DO 331 I=1,IE
      DO 330 K=3,KN
      EX=(KA(I,K)+KA(I,K+1))/2.
  330 HC(I,K)=EX
```

```
      HC(I,2)=.16*SQRT(U(I,2)**2+V(I,2)**2)*ZA(2)/ALOG((ZA(2)+ZO)/ZO)
      HC(I,1)=0.
  331 HC(I,KE)=HC(I,KN)
      CALL PRNT(HC,FMTH)
C
      IF(IP .EQ. 0) GO TO 95
C
C     RADIATIVE FLUX OUTPUT
C
      WRITE(6,3600)
      DO 340 I=1,IE
      DO 340 K=1,KE
      HR=RF*SIGMA*(T(I,1)**4)*EXP(-INT(I,KE)+INT(I,K))*60.
  340 HC(I,K)=HR
      CALL PRNT(HC,FMTH)
C
C     RADIATIVE COOLING RATE OUTPUT
C
      WRITE(6,3700)
      DO 350 I=1,IE
      DO 350 K=1,KE
      COOL=-3600.*(W(I,K)**.667)*CR*(T(I,1)**4.)*EXP(-INT(I,KE)+INT(I,K)
     1)*CP/CPT(I,K)
  350 HC(I,K)=COOL
      CALL PRNT(HC,FMTH)
C
C     WATER VAPOR FLUX OUTPUT
C
      WRITE(6,3800)
      DO 361 I=1,IE
      DO 360 K=3,KN
      HC(I,K)=-DEN*.5*((KA(I,K+1)*(R(I,K+1)-R(I,K))/(ZA(K+1)-ZA(K)))+(KA
     1(I,K)*(R(I,K)-R(I,K-1))/(ZA(K)-ZA(K-1))))
  360 CONTINUE
      WINDV2=SQRT(U(I,2)**2+V(I,2)**2)
      HC(I,2)=-DEN*.16*WINDV2*(R(I,2)-R(I,1))/(ALOG((ZA(2)+ZO)/ZO)**2)
      HC(I,1)=HC(I,2)
       HC(I,KE)=HC(I,KN)
  361  CONTINUE
      CALL PRNT(HC,FMTH)
C
C     VERTICAL VELOCITY OUTPUT
C
      WRITE(6,3900)
      DO 370 I=1,IE
      DO 370 K=1,KE
  370 HC(I,K)=WINT(I,K)
      CALL PRNT(HC,FMTH)
      GO TO 95
  400 STOP
 1000 FORMAT(10E8.2)
 1100 FORMAT(14I5)
 1200 FORMAT(3E10.3,6I5,-2PF6.0)
 1205 FORMAT(11A4/11A4)
 1300 FORMAT(4E10.3)
 1400 FORMAT(8F10.2)
 1500 FORMAT(6E10.3)
 2000 FORMAT(1H1,////,60X,10HINPUT DATA,//,1H0,1P10E10.3)
 2100 FORMAT(1H0,14I5)
 2200 FORMAT(1H0,1P3E10.3,0P6I5,-2PF6.0)
 2300 FORMAT(1H0,4E10.3)
```

```
 2400 FORMAT(1H0,8F10.2)
 2500 FORMAT(1H0,8E10.3)
 3000 FORMAT(30H1EDDY HEAT FLUX IN WATTS/CM**2///)
 3008 FORMAT(28H1FRICTION VELOCITY IN CM/SEC///)
 3009 FORMAT(29H1U COMPONENT OF WIND IN M/SEC///)
 3010 FORMAT(29H1V COMPONENT OF WIND IN M/SEC///)
 3100 FORMAT(21H1TEMPERATURE IN DEG K///)
 3200 FORMAT(20H1MIXING RATIO IN G/G///)
 3300 FORMAT(31H1LIQUID WATER CONTENT IN G/M**3///)
 3400 FORMAT(30H1DEW POINT DEPRESSION IN DEG C///)
 3410 FORMAT(33H1TURBULENT ENERGY IN CM**2/SEC**2///)
 3500 FORMAT(44H1TURBULENT EXCHANGE COEFFICIENT IN CM**2/SEC///)
 3600 FORMAT(31H1RADIATIVE FLUX IN CAL/CM**2MIN///)
 3700 FORMAT(30H1RADIATIVE COOLING IN DEG C/HR///)
 3800 FORMAT(34H1EDDY MOISTURE FLUX IN G/CM**2 SEC///)
 3900 FORMAT(28H1VERTICAL VELOCITY IN CM/SEC///)
 4000 FORMAT(10Z8)
 5000 FORMAT(5Z16)
      END
C
C     INTEGRATION SUBROUTINE
C
C     INTEGRATE ONE TIME STEP AND COMPUTE NEW PROGNOSTIC & DIAGNOSTIC
C     VARIABLES
C
      SUBROUTINE STEP
       REAL*8 PT,EPT,FPT,DPT,AT,CT,BT
      REAL*4 KA,INT,KW,L,LM,LMAX,KM,LMM
      COMMON PT(40,60),EPT(60),FPT(60),DPT,AT,CT,BT,
     8     WINT(40,60),R(40,60),W(40,60),U(40,60),T(40,60),KA(40,60),
     7KM(40,60),LM(60),LMM(60),Q(40,60),EQ(60),FQ(60),
     1       INT(40,60),CPT(40,60),HC(40,60),X(40),DX(40),DTEM(40),
     2       P(60),ZA(60),DZA(60),                    ER(60),FR(60),EW(60),
     3       FW(60),EU(60),FU(60),Z(60),DZ(60),PR(60),L,DEN,CP,G,RA,RW,
     4       SIGMA,TIME,DT,TIM,UF,RF,KW,ZO,CV,UI,DTEMI,ZAK,XAI,DELX,CC,
     5       CH,CI,CK,CL,CR,CS,UU,FV(60),EV(60),V(40,60),     F,
     6       KL,KN,IE,IN,IL,IR,ISED,IRAD,IRSFC,IDTEM,ITEML,ITEMR,IP,II
C
C     UPWIND DO LOOP OVER HORIZONTAL GRID SYSTEM
C
      DO 80 M=2,IN
      I=IN+2-M
C
C     DOWNWARD DO LOOP OVER VERTICAL GRID SYSTEM TO SET UP IMPLICIT
C     INTEGRATION
C
      DO 20 N=2,KN
      K=KN+2-N
    5 DD=DT/DZ(K)
      A=DD*KA(I,K+1)*DZA(K)/DZA(K+1)
      AT=A
      ARR=A
      AW=A
      AU=DD*KM(I,K+1)*DZA(K)/DZA(K+1)
      AUU=II*AU
      AQ=      AU
      DQT=8.*LM(K)/(SQRT(Q(I,K))*DT)
      IF(KM(I,K) .LT. .21) DQT=1.
      AQ=AQ*DQT
      C=DD*KA(I,K)
      CT=C
```

```
      CRR=C
      CW=C
      CU=DD*KM(I,K)
      CUU=II*CU
      CQ=      CU
      CQ=CQ*DQT
C
   10 B=1.+A+C
      BT=1.+AT+CT
      BUU=1.+AUU+CUU
      BRR=1.+ARR+CRR
      BW=B
      BQ=1.+AQ+CQ
      IF(ISED .NE.1) GO TO 11
C
C     DROP SEDIMENTATION
C
      DS=DT*CV/DZA(K+1)
      AW=AW+DS*(W(I,K+1)**.667)
      BW=BW+DS*W(I,K)**.667
C
   11 DPT=PT(I,K)-U(I,K)*(PT(I,K)-PT(I-1,K))*DT/DX(I)
C     RADIATIONAL COOLING
C
      IF((IRAD .EQ. 1) .AND. (W(I,K) .GT. 0.0)) DPT=DPT-CR*W(I,K)*(PT(I,
     11)**4.)*EXP(-INT(I,KE)+INT(I,K))*PR(K)*DT/(W(I,K)**.333)
C
       DU=U(I,K)*(1.+(II-1)*(AU+CU))-(II-1)*(AU*U(I,K+1)+CU*U(I,K-1))
     1-U(I,K)*(U(I,K)-U(I-1,K))*DT/DX(I) + F*(V(I,K)-V(I,KE))*DT
       DV=V(I,K)*(1.+(II-1)*(AU+CU))-(II-1)*(AU*V(I,K+1)+CU*V(I,K-1))
     1-U(I,K)*(V(I,K)-V(I-1,K ))*DT/DX(I) + F*(U(I,KE)-U(I,K))*DT
      DR  = R(I,K)-U(I,K)*( R(I,K)- R(I-1,K))*DT/DX(I)
      DW  = W(I,K)-U(I,K)*( W(I,K)- W(I-1,K))*DT/DX(I)
      DQ=       -U(I,K)*(Q(I,K)-Q(I-1,K))*DT/DX(I)
      DWZ=SQRT((U(I,K)-U(I,K-1))**2+(V(I,K)-V(I,K-1))**2)/DZA(K)
      IF(W(I,2) .GT. 0.) GO TO 13
      S=(PT(I,2)-PT(I,2-1))/DZA(2)
      GO TO 14
   13 S=(T(I,2)-T(I,2-1))/DZA(2)+CS/CPT(I,2)
   14 DQ=DQ+DT*(.25*Q(I,1)*DWZ - KM(1,2)*G*S/PT(1,1))
      DQ=DQ*DQT
      IF(KM(I,K) .LT. .21) DQ=DQ+Q(I,K)-(Q(I,K)**1.5)*DT/(8.*LM(K))
   16 EU(K)=CUU/(BUU-AUU*EU(K+1))
      EV(K)=CUU/(BUU-AUU*EV(K+1))
      EPT(K)=CT/(BT-AT*EPT(K+1))
      ER(K)=CRR/(BRR-ARR*ER(K+1))
      EW(K)=CW/(BW-AW*EW(K+1))
      EQ(K)=CQ/(BQ-AQ*EQ(K+1))
      FU(K)=(DU+AUU*FU(K+1))*EU(K)/CUU
      FV(K)=(DV+AUU*FV(K+1))*EV(K)/CUU
      FPT(K)=(DPT+AT*FPT(K+1))*EPT(K)/CT
      FR(K)=(DR+ARR*FR(K+1))*ER(K)/CRR
      FW(K)=(DW+AW*FW(K+1))*EW(K)/CW
      FQ(K)=(DQ+AQ*FQ(K+1))*EQ(K)/CQ
   20 CONTINUE
C
C     UPDATE SURFACE BOUNDARY CONDITION
C
      IF(TIME .LE. TIM) PT(I,1)=PT(1,1)+DTEM(I)*TIME/TIM
      IF(TIME .LE. TIM) T(I,1)=PT(I,1)
      IF(IRSFC .EQ. 0) R(I,1)=FR(2)/(1.-ER(2))
```

```
C
C     SATURATION SURFACE BOUNDARY CONDITION ON R
C
      IF(IRSFC  .EQ. 1) R(I,1)=RSF(T(I,1),1000.)
C
C     UPWARD DO LOOP OVER VERTICAL GRID SYSTEM TO COMPUTE NEW PROGNOSTIC
C     AND DIAGNOSTIC VARIABLES
C
      INT(I,1)=0.0
      DO 70 K=2,KE
      IF(K .EQ. KE) GO TO 40
      U(I,K)=EU(K)*U(I,K-1)+FU(K)
      V(I,K)=EV(K)*V(I,K-1)+FV(K)
      PT(I,K)=EPT(K)*PT(I,K-1)+FPT(K)
      R(I,K)=ER(K)*R(I,K-1)+FR(K)
      W(I,K)=EW(K)*W(I,K-1)+FW(K)
   25 Q(I,K)=EQ(K)*Q(I,K-1)+FQ(K)
      IF(K .EQ. 2) Q(I,2)=Q(I,1)
      IF(Q(I,K) .LE. 0.) GO TO 27
      IF(.5*SQRT(Q(I,K))*LM(K) .LT. .2) GO TO 27
      GO TO 26
   27 Q(I,K)=.16/(LM(K)**2)
C
C     COMPUTE TEMPERATURE
C
   26 T(I,K)=PT(I,K)/PR(K)
C
C     SATURATION ADJUSTMENT
C
      RS=RSF(T(I,K),P(K))
      IF((R(I,K) .LE. RS) .AND. (W(I,K) .LE. 0.0)) GO TO 40
      DR=(R(I,K)-RS)/(1.+CC*RS/(T(I,K)**2))
      IF(R(I,K) .GT. RS) GO TO 30
      IF(-DR .LE. W(I,K)) GO TO 30
      DR=-W(I,K)
   30 T(I,K)=T(I,K)+DR*L/CP
      PT(I,K)=T(I,K)*PR(K)
      R(I,K)=R(I,K)-DR
      W(I,K)=W(I,K)+DR
C
C     COMPUTE NEW VALUES OF INT, CPT, AND KA
C
   40 IF(W(I,K) .LT. 0.0) W(I,K)=0.0
      INT(I,K)=INT(I,K-1)+CI*DZA(K)*W(I,K)**.667
      DWZ=SQRT((U(I,K)-U(I,K-1))**2+(V(I,K)-V(I,K-1))**2)/DZA(K)
      IF(W(I,K) .GT. 0.0) GO TO 50
      CPT(I,K)=CP
      GO TO 60
   50 CPT(I,K)=CP+CH*RSF(T(I,K),P(K))/(T(I,K)**2)
   60 IF(K .EQ. 2) GO TO 71
C
C     DIAGNOSIS OF EXCHANGE COEFFICIENTS COVERING NEUTRAL,STABLE AND
C     UNSTABLE CONDITIONS BETWEEN K=2 AND THE SURFACE
C
      QM=Q(I,K)
      KM(I,K)=.50*SQRT(QM)*LM(K)
      KA(I,K)=KM(I,K)
      GO TO 70
   71 KM(I,2)=.16*DWZ*DZA(2)**2/(ALOG((ZA(2)+Z0)/Z0)**2)
      KA(I,2)=KM(I,2)
      Q(I,1)=4.*KM(I,2)*DWZ
```

```
C
   70 CONTINUE
C
C     UPDATE SURFACE BOUNDARY CONDITION ON R AFTER SATURATION ADJUSTMENT
C     IF NO FLUX CONDITION USED
C
      IF(IRSFC .EQ. 0) R(I,1)=R(I,2)
C
   80 CONTINUE
C
C     UPDATE DOWNWIND BOUNDARY CONDITION
C
      DO 90 K=1,KE
   90 CONTINUE
      DO 102 I=2,IN
      DO 99 K=2,KE
   99 WINT(I,K)=WINT(I,K-1)-(U(I,K)-U(I-1,K))*DZA(K)/DX(I)
  102 CONTINUE
      RETURN
      END
C
C
C
C     PRINT SUBROUTINE
C
      SUBROUTINE PRNT(O,FORM)
      REAL*8 PT,EPT,FPT,DPT,AT,CT,BT
      REAL*4 KA,INT,KW,L,LM,LMAX,KM,LMM
      COMMON PT(40,60),EPT(60),FPT(60),DPT,AT,CT,BT,
     8     WINT(40,60),R(40,60),W(40,60),U(40,60),T(40,60),KA(40,60),
     7KM(40,60),LM(60),LMM(60),Q(40,60),EQ(60),FQ(60),
     1        INT(40,60),CPT(40,60),HC(40,60),X(40),DX(40),DTEM(40),
     2        P(60),ZA(60),DZA(60),                    ER(60),FR(60),EW(60),
     3        FW(60),EU(60),FU(60),Z(60),DZ(60),PR(60),L,DEN,CP,G,RA,RW,
     4        SIGMA,TIME,DT,TIM,UF,RF,KW,ZO,CV,UI,DTEMI,ZAK,XAI,DELX,CC,
     5        CH,CI,CK,CL,CR,CS,UU,FV(60),EV(60),V(40,60),     F,
     6        KE,KN,IE,IN,IL,IR,ISED,IRAD,IRSFC,IDTEM,ITEML,ITEMR,IP,II
      DIMENSION O(40,60),FORM(11)
C
C     OUTPUT DOCUMENTATION
C
      WRITE(6,4000) TIME,DTEMI,ITEML,ITEMR
C
C     PAGE 1 COLUMNS 1-10
C
      I2=10
      IF(IE .LT. 10) I2=IE
      WRITE(6,4100) (X(I),I=1,I2)
      DO 450 J=1,KE
      K=KE-J+1
  450 WRITE(6,FORM) ZA(K),(O(I,K),I=1,I2)
C
      IF(IE .LT. 11) GO TO 490
C
C     PAGE 2 COLUMNS 11-20
C
      WRITE(6,4105) (X(I),I=11,20)
      DO 460 J=1,KE
      K=KE-J+1
  460 WRITE(6,FORM) ZA(K),(O(I,K),I=11,20)
C
```

```
      IF(IE .LT. 21) GO TO 490
C
C     PAGE 3 COLUMNS 21-30
C
      WRITE(6,4105) (X(I),I=21,30)
      DO 470 J=1,KE
      K=KE-J+1
  470 WRITE(6,FORM) ZA(K),(O(I,K),I=21,30)
C
      IF(IE .LT. 31) GO TO 490
C
C     PAGE 4 COLUMNS 31-IE
C
      WRITE(6,4105) (X(I),I=31,IE)
      DO 480 J=1,KE
      K=KE-J+1
  480 WRITE(6,FORM) ZA(K),(O(I,K),I=31,IE)
C
  490 CONTINUE
 4000 FORMAT(6HOTIME=,F7.0,4H SEC,6X,6HDTEMI=,F5.1,2H K,6X,6HITEML=,I2,2
     1X,6HITEMR=,I2)
 4100 FORMAT(1HO,6HX(KM)=,6X,10(-5PF12.2) / 1H ,3X,5HZ(CM))
 4105 FORMAT(1H1,6HX(KM)=,6X,10(-5PF12.2) / 1H ,3X,5HZ(CM))
      RETURN
      END
C
C
C     SATURATION MIXING RATIO AS A FUNCTION OF TEMPERATURE A AND
C     PRESSURE B
C
      FUNCTION RSF(A,B)
      ES=6.1078*EXP(17.26939*(A-273.16)/(A-35.86))
      RSF=.62465*ES/(B-ES)
      RETURN
      END
C
C
```